The MFS for the detection of inner boundaries in linear elasticity

A. Karageorghis[1], D. Lesnic[2] & L. Marin[3]
[1] *Department of Mathematics and Statistics, University of Cyprus, Nicosia, Cyprus*
[2] *Department of Applied Mathematics, University of Leeds, UK*
[3] *Institute of Solid Mechanics, Romanian Academy, Bucharest, Romania*

Abstract

We propose a nonlinear minimization method of fundamental solutions for the detection (shape, size and location) of unknown inner boundaries corresponding to either a rigid inclusion or a cavity inside a linear elastic body from nondestructive boundary measurements of displacement and traction. The stability of the numerical method is investigated by inverting measurements contaminated with noise.
Keywords: Cauchy–Navier equations, method of fundamental solutions, regularization.

1 Introduction

The method of fundamental solutions (MFS) [1, 2] is a meshless boundary collocation method [3] which may be used for the numerical solution of certain boundary value problems. The method has become increasingly popular over the last three decades primarily because of the ease with which it can be implemented. A comparison between the MFS and the boundary element method (BEM), as applied to direct problems, has been performed in [4]. In recent years, the MFS has been used extensively for the numerical solution of inverse problems primarily. An extensive survey of the applications of the MFS to inverse problems is provided in [5]. The most difficult class of inverse problems are the so-called *inverse geometric problems* in which the location and shape of part of the boundary of the domain of the problem in question are unknown and need to be calculated as part of the solution. The MFS was used for the first time for the solution of inverse geometric


WIT Transactions on Modelling and Simulation, Vol 52, © 2011 WIT Press
www.witpress.com, ISSN 1743-355X (on-line)
doi:10.2495/BE110201

problems in linear elasticity in [6], while more recent applications may be found in [7, 8].

2 Mathematical formulation

In practical nondestructive evaluation (testing) of materials the following inverse problem naturally arises: Given an elastic body Ω, detect an unknown inclusion $D \subset \Omega$ from measurements of the traction and displacement taken on the boundary $\partial\Omega$. This situation commonly arises, for instance, in fracture mechanics when some defects stem from the manufacturing process, or when the elastic properties of the material deteriorate due to the occurrence of possible damage [9].

In mathematical terms, and considering, for simplicity, a two-dimensional isotropic and homogeneous elastic simply-connected bounded body $\Omega \subset \mathbb{R}^2$, our goal is to determine the displacement $\mathbf{u} = (u_1, u_2)$ and an inclusion D compactly contained in Ω, i.e. $\overline{D} \subset \Omega$, such that $\Omega \backslash D$ is connected, satisfying the Cauchy–Navier equations (Lamé system) of elasticity

$$\begin{cases} G\left(\dfrac{\partial^2 u_1}{\partial x^2} + \dfrac{\partial^2 u_1}{\partial y^2}\right) + \dfrac{G}{1-2\overline{\nu}}\left(\dfrac{\partial^2 u_1}{\partial x^2} + \dfrac{\partial^2 u_2}{\partial x \partial y}\right) = 0, \quad \text{in } \Omega\backslash\overline{D}, \\ G\left(\dfrac{\partial^2 u_2}{\partial x^2} + \dfrac{\partial^2 u_2}{\partial y^2}\right) + \dfrac{G}{1-2\overline{\nu}}\left(\dfrac{\partial^2 u_1}{\partial x \partial y} + \dfrac{\partial^2 u_2}{\partial y^2}\right) = 0, \quad \text{in } \Omega\backslash\overline{D}, \end{cases} \tag{1a}$$

subject to the Cauchy boundary conditions on the outer boundary $\partial\Omega$

$$u_i = f_i, \quad i = 1, 2 \text{ on } \partial\Omega, \tag{1b}$$

$$t_i = g_i, \quad i = 1, 2 \text{ on } \partial\Omega, \tag{1c}$$

and either homogeneous Dirichlet conditions

$$u_i = 0, i = 1, 2 \quad \text{on} \quad \partial D, \tag{1d}$$

or homogeneous Neumann conditions

$$t_i = 0, \quad i = 1, 2 \text{ on } \partial D, \tag{1e}$$

on the inner boundary ∂D. Here f_i and $g_i, i = 1, 2$ are known displacements and tractions, respectively, G is the shear modulus, $\overline{\nu} = \nu$ in the plane strain state and $\overline{\nu} = \nu/(1+\nu)$ in the plane stress state, where ν is Poisson's ratio. According to [6], the homogeneous Dirichlet conditions (1d) on the inner boundary ∂D physically describe a rigid inclusion, while the homogeneous Neumann conditions (1e) on ∂D characterise a cavity.

The strain tensor $\boldsymbol{\varepsilon} = (\varepsilon_{ij})_{i,j=1,2}$ is related to the displacements by the kinematic relations, i.e.

$$\boldsymbol{\varepsilon} = \begin{bmatrix} \dfrac{\partial u_1}{\partial x} & \dfrac{1}{2}\left(\dfrac{\partial u_1}{\partial y} + \dfrac{\partial u_2}{\partial x}\right) \\ \dfrac{1}{2}\left(\dfrac{\partial u_1}{\partial y} + \dfrac{\partial u_2}{\partial x}\right) & \dfrac{\partial u_2}{\partial y} \end{bmatrix}, \tag{2}$$

while the stress tensor $\boldsymbol{\sigma} = (\sigma_{ij})_{i,j=1,2}$ is related to the elements of the strain tensor according to Hooke's law by

$$\boldsymbol{\sigma} = 2G \begin{bmatrix} \varepsilon_{11} + \dfrac{\overline{\nu}}{1-2\overline{\nu}}(\varepsilon_{11}+\varepsilon_{22}) & \varepsilon_{12} \\ \varepsilon_{21} & \varepsilon_{22} + \dfrac{\overline{\nu}}{1-2\overline{\nu}}(\varepsilon_{11}+\varepsilon_{22}) \end{bmatrix}. \tag{3}$$

Finally, the tractions $t_i, i = 1, 2$ in (1c) are defined by $[t_1, t_2]^T = \boldsymbol{\sigma}\boldsymbol{n}$, where $\boldsymbol{n} = [n_1, n_2]^T$ denotes the outward normal vector to the boundary. Equations (1a) may be written more compactly as $\nabla \cdot \boldsymbol{\sigma} = \mathbf{0}$.

Note that the boundary $\partial\Omega$ is overspecified since both the displacements and tractions are prescribed on it through equations (1b) and (1c). Consequently, we cannot expect that a solution to the above inverse problem exists for arbitrary Cauchy data $\mathbf{f}$ and $\mathbf{g}$. However, the following uniqueness result holds.

Theorem. [6] *Let $\overline{D} \subset \Omega \subset \mathbb{R}^2$ be open, bounded and simply connected domains with smooth boundaries such that the domain of elastic propagation $\Omega\backslash D$ is connected. Let also the Dirichlet and Neumann data $\mathbf{f}$ and $\mathbf{g}$ in* (1b) *and* (1c) *be such that $\mathbf{f} \in [H^{1/2}(\partial\Omega)]^2$ and $\mathbf{g} \in [H^{-1/2}(\partial\Omega)]^2$.*

(i) If $\mathbf{f} \not\equiv \mathbf{0}$ then a single pair of Cauchy data $(\mathbf{f}, \mathbf{g})$ determines (identifies) uniquely the displacement $\mathbf{u} \in [H^1(\Omega\backslash D)]^2$ and the rigid inclusion D satisfying the inverse Dirichlet problem given by equations (1a)-(1d)*.*

(ii) If $\mathbf{f} \notin span\{(1,0),(0,1),(-y,x)\}_{(x,y)\in\partial\Omega}$ then a single pair of Cauchy data $(\mathbf{f}, \mathbf{g})$ determines (identifies) uniquely the displacement $\mathbf{u} \in [H^1(\Omega\backslash D)]^2$ and the cavity D satisfying the inverse Neumann problem given by equations (1a)-(1c) *and* (1e)*.*

Remarks:

(a) The condition in (ii) above says that $\mathbf{f}$ does not belong to the linear space of rigid displacements on $\partial\Omega$ and it can be replaced by the condition $\mathbf{g} \not\equiv \mathbf{0}$.

(b) The inverse inclusion problems under investigations are further ill-posed because they are unstable, i.e. small noisy errors in the input data (1b) and/or (1c) cause large errors in the solution $(\mathbf{u}, D)$.

3 The method of fundamental solutions (MFS)

We approximate the displacements $u_i, i = 1, 2$ by the MFS approximations [6–8]

$$u_i^N(\boldsymbol{x}, \boldsymbol{\xi}; \boldsymbol{\alpha}, \boldsymbol{\beta}) = \sum_{j=1}^{2N} \alpha_j U_{i1}(\boldsymbol{x}, \boldsymbol{\xi}_j) + \sum_{j=1}^{2N} \beta_j U_{i2}(\boldsymbol{x}, \boldsymbol{\xi}_j), \quad \boldsymbol{x} \in \overline{\Omega} \backslash D, \tag{4}$$

where $\boldsymbol{\xi} = (\boldsymbol{\xi}_j)_{j=\overline{1,N}}$ are the singularities located in D while $\boldsymbol{\xi} = (\boldsymbol{\xi}_j)_{j=\overline{N+1,2N}}$ are the singularities located outside $\overline{\Omega}$. The vectors $\boldsymbol{\alpha} = (\alpha_j)_{j=1,\ldots,2N}$, $\boldsymbol{\beta} = (\beta_j)_{j=1,\ldots,2N}$ contain unknown real coefficients to be determined. The displacement fundamental solution matrix $U = (U_{ij})_{i,j=1,2}$ associated with the points $\boldsymbol{x} = (x, y)$ and $\boldsymbol{\xi} = (\xi_x, \xi_y)$ is given in [10].

On combining the kinematic relations (2), Hooke's law (3) and the MFS approximations for the displacements (4), the following MFS approximations for the tractions $t_i, i = 1, 2$ are obtained

$$t_i^N(\boldsymbol{x}, \boldsymbol{\xi}; \boldsymbol{\alpha}, \boldsymbol{\beta}) = \sum_{j=1}^{2N} \alpha_j T_{i1}(\boldsymbol{x}, \boldsymbol{\xi}_j) + \sum_{j=1}^{2N} \beta_j T_{i2}(\boldsymbol{x}, \boldsymbol{\xi}_j), \quad \boldsymbol{x} \in \partial\Omega \cup \partial D, \tag{5}$$

where the traction fundamental solution matrix $T = (T_{ij})_{i,j=1,2}$ is given in, e.g. [10].

3.1 Parametrization of the unknown boundary and choice of the boundary collocation and source points

Without loss of generality, we assume that the known outer boundary $\partial\Omega$ is a circle of radius r_o. Then, the outer boundary collocation and source points can be chosen as

$$\boldsymbol{x}_{N+k} = r_o(\cos(\vartheta_k), \sin(\vartheta_k)), \ \boldsymbol{\xi}_{N+k} = \eta_o r_o(\cos(\vartheta_k), \sin(\vartheta_k)), \ k = \overline{1, N}, \tag{6}$$

where $\vartheta_k = 2\pi(k-1)/N$, $k = \overline{1, N}$, and $\eta_o > 1$ is fixed.

We further assume that the unknown rigid inclusion or cavity D is a star-shaped domain with respect to the origin. The more general case in which the center of the star-shaped domain D is unknown can also be investigated with no major modifications, see [11]. Thus we can parameterize the boundary ∂D as

$$x = r(\vartheta)\cos\vartheta, \quad y = r(\vartheta)\sin\vartheta, \quad \vartheta \in [0, 2\pi), \tag{7}$$

where r is a $2\pi-$periodic function. The collocation form of (7) in two dimensions becomes

$$r_k = r(\vartheta_k), \quad k = \overline{1, N}, \tag{8}$$

and we choose the inner boundary and source points as

$$\boldsymbol{x}_k = r_k(\cos\vartheta_k, \sin\vartheta_k), \quad \boldsymbol{\xi_k} = \eta_{int}\boldsymbol{x}_k, \quad k = \overline{1, N}, \tag{9}$$

where $\eta_{int} \in (0, 1)$ is fixed.

3.2 Penalized least-squares minimization

The coefficients $\boldsymbol{\alpha} = (\alpha_j)_{j=\overline{1,2N}}$, $\boldsymbol{\beta} = (\beta_j)_{j=\overline{1,2N}}$ and the radii $\boldsymbol{r} = (r_j)_{j=\overline{1,N}}$ can be determined by imposing the boundary conditions (1b)-(1d), or (1b), (1c) and (1e). We thus have a total of $6N$ equations in $5N$ unknowns. Note that the inverse inclusion problem under investigation is linear in the coefficients $\boldsymbol{\alpha}$ and $\boldsymbol{\beta}$, but it is nonlinear in the radii $\boldsymbol{r}$.

In the case of the inverse geometric problem (1a)-(1d) associated with the detection of the unknown rigid inclusion D, the penalized least-squares functional to be minimized is given by the sum of the residual and the regularization terms, namely,

$$\begin{aligned} S(\boldsymbol{\alpha},\boldsymbol{\beta},\boldsymbol{r}) &= Res(\boldsymbol{\alpha},\boldsymbol{\beta},\boldsymbol{r}) + Reg(\boldsymbol{\alpha},\boldsymbol{\beta},\boldsymbol{r}) \\ &= \sum_{i=1}^{2}\sum_{j=1}^{2N}\left[u_i^N(\boldsymbol{x}_j,\boldsymbol{\xi};\boldsymbol{\alpha},\boldsymbol{\beta}) - f_i(\boldsymbol{x}_j)\right]^2 \\ &\quad + \sum_{i=1}^{2}\sum_{j=N+1}^{2N}\left[t_i^N(\boldsymbol{x}_j,\boldsymbol{\xi};\boldsymbol{\alpha},\boldsymbol{\beta}) - g_i(\boldsymbol{x}_j)\right]^2 \\ &\quad + \mu_1\left(|\boldsymbol{\alpha}|^2 + |\boldsymbol{\beta}|^2\right) + \mu_2\sum_{\ell=2}^{N}(r_\ell - r_{\ell-1})^2, \end{aligned} \tag{10}$$

where $f_i(\boldsymbol{x}_j) \equiv 0$ for $i = 1, 2$ and $j = \overline{1,N}$, and $\mu_1, \mu_2 > 0$ are regularization parameters. The functional (10) is minimized subject to the simple bounds on the variables

$$0 < r_m < r_o, \quad m = \overline{1,N}. \tag{11}$$

In (10), the last two terms, included in order to achieve stability, correspond to penalising the ℓ^2-norm of the coefficients $\boldsymbol{\alpha}$ and $\boldsymbol{\beta}$, and the H^1-discretised norm of the smooth obstacle radii $\boldsymbol{r}$.

The Cauchy data given on $\partial\Omega$ in the boundary conditions (1b) and (1c) come from practical measurements which are inherently contaminated with noisy errors, and therefore we replace f_i and g_i by f_i^p and g_i^p, $i = 1, 2$, respectively, generated as

$$f_i^p(\boldsymbol{x}_j) = (1 + \rho_j^f p_{\boldsymbol{u}})f_i(\boldsymbol{x}_j), \quad i = 1, 2,\ j = \overline{N+1,2N}, \tag{12}$$

$$g_i^p(\boldsymbol{x}_j) = (1 + \rho_j^g p_{\boldsymbol{t}})g_i(\boldsymbol{x}_j), \quad i = 1, 2,\ j = \overline{N+1,2N}, \tag{13}$$

where $p_{\boldsymbol{u}}$ and $p_{\boldsymbol{t}}$ represent the percentage of noise added into the displacements and tractions on $\partial\Omega$, respectively, and $\left(\rho_j^f\right)_{j=\overline{N+1,2N}}$ and $\left(\rho_j^g\right)_{j=\overline{N+1,2N}}$ are pseudo-random noisy variables drawn from a uniform distribution on $[-1, 1]$ using the NAG [12] routine `G05DAF`. Since the inverse problem under investigation is ill-posed being unstable, i.e. small errors $p_{\boldsymbol{u}}$ and/or $p_{\boldsymbol{t}}$ in the data (12) and/or (12) cause large errors in the solution for ∂D, the C^1-smoothness regularization term

involving μ_2 was added in order to achieve stability. In addition, the regularization term involving μ_1 was added in order to deal with the ill-conditioned MFS system of equations.

The minimization of (10) is carried out using the `MINPACK` routine `lmdif` which minimizes the unconstrained sum of squares of nonlinear functions. The simple bound constraints (11) are imposed during the iterative procedure by adjustment at each iteration. The initial guess for the unknowns has been taken arbitrarily to be $\boldsymbol{\alpha}^{(0)} = \boldsymbol{\beta}^{(0)} = \mathbf{0}$ and $\boldsymbol{r}^{(0)} = 1$. The Jacobian is calculated internally using forward finite differences.

3.3 Regularization

In order to obtain a stable solution, regularization of the numerical solution can be accomplished by one of the following two approaches. In a first instance, if no regularization terms are included in the objective functional (10), i.e. $\mu_1 = \mu_2 = 0$, then, according to the discrepancy principle, we stop the iterations involved in the process of minimization once the residual $Res(\boldsymbol{\alpha}, \boldsymbol{\beta}, \boldsymbol{r})$ becomes less than the amount of noise, i.e.

$$Res(\boldsymbol{\alpha}, \boldsymbol{\beta}, \boldsymbol{r}) \leq \epsilon := \sum_{i=1}^{2} \sum_{j=N+1}^{2N} \left\{ [f_i^p(\boldsymbol{x}_j) - f_i(\boldsymbol{x}_j)]^2 + [g_i^p(\boldsymbol{x}_j) - g_i(\boldsymbol{x}_j)]^2 \right\}. \tag{14}$$

However, we do not know whether the minimization routine `lmdif` which is employed has a regularization character which justifies this stopping criterion. In order to add some rigour into the stability of the numerical solution, we consider next including some positive regularization parameters μ_1 and μ_2 in (10). Then the iteration process does not need to be stopped, i.e. it can be left to run until a user specified tolerance, say of 10^{-10}, is achieved or a maximum number of function evaluations, `maxfev`, is reached. However, one still has to choose appropriately the regularization parameters μ_1 and μ_2 and this can be done either based on the above discrepancy principle, or on the more heuristic L-curve or L-surface criterion, see [13, 14].

4 Numerical example

We consider an example for which an analytical solution is available (see [8]) in order to assess the accuracy and stability of the proposed method. In particular, we consider an isotropic linear elastic medium, e.g. copper alloy, characterised by the material constants $\bar{\nu} = \nu = 0.34$ and $G = 3.35 \times 10^{10}\,\mathrm{N/m^2}$, and occupying the two-dimensional annular domain $\Omega \setminus \overline{D}$, where

$$\Omega = \left\{(x, y) \in \mathbb{R}^2 | x^2 + y^2 < r_o^2\right\}, \; D = \left\{(x, y) \in \mathbb{R}^2 | x^2 + y^2 < r_{int}^2\right\}, \tag{15}$$

where $0 < r_{int} < r_o$. We also consider the following exact solution for the displacements

$$u_1(x,y) = \frac{1}{2G(1+\nu)}\left[V(1-\nu) - W(1+\nu)\frac{1}{(x^2+y^2)}\right]x, \tag{16}$$

$$u_2(x,y) = \frac{1}{2G(1+\nu)}\left[V(1-\nu) - W(1+\nu)\frac{1}{(x^2+y^2)}\right]y, \tag{17}$$

where $(x,y) \in \overline{\Omega}\backslash D$ and

$$V = -\frac{\sigma_o r_o^2 - \sigma_{int} r_{int}^2}{r_o^2 - r_{int}^2}, \quad W = \frac{(\sigma_o - \sigma_{int}) r_o^2 r_{int}^2}{r_o^2 - r_{int}^2}, \quad \sigma_o, \sigma_{int} \in \mathbb{R}. \tag{18}$$

The corresponding stress tensor is given by

$$\sigma_{ij}(\boldsymbol{x}) = \left[V + (-1)^{i+1} W \frac{x^2 - y^2}{(x^2+y^2)^2}\right]\delta_{ij} + 2W\frac{xy}{(x^2+y^2)^2}(1-\delta_{ij}), i,j = 1,2. \tag{19}$$

By choosing

$$\sigma_o = \left[(1+\nu) + (1-\nu)\frac{r_{int}^2}{r_o^2}\right]\frac{\sigma_{int}}{2}, \quad \sigma_{int} = 1.0 \times 10^{10}\,\mathrm{N/m^2},$$

in expressions (16)-(19), we have that $u_1 = u_2 = 0$ on the inner boundary of the circular rigid inclusion ∂D. For these dimensional quantities, in order to have the

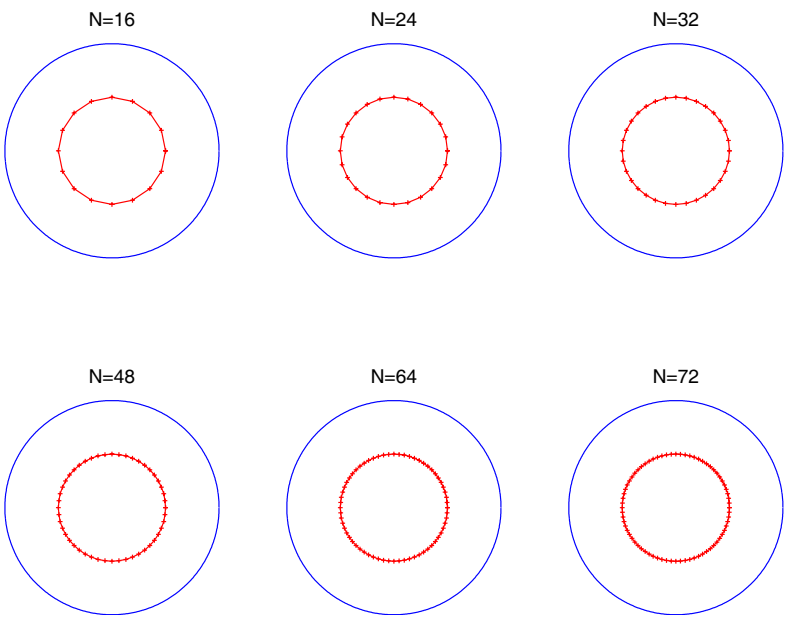

Figure 1: Results for various N with no noise and no regularization.

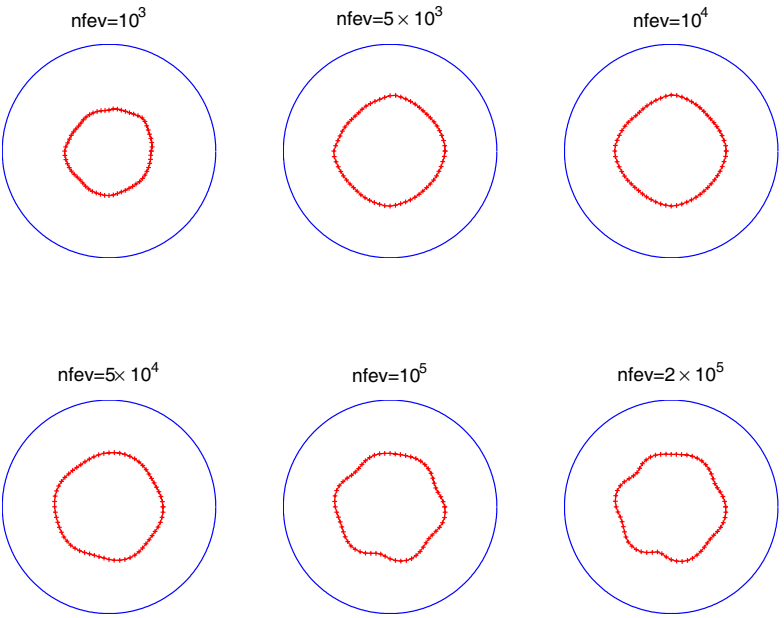

Figure 2: Results for various values of nfev with $p_{\boldsymbol{t}} = 5\%$ noise and no regularization.

first two terms to be minimized in (10) of the same order of magnitude, we weigh the second term accordingly.

We conducted numerical experiments with $r_{int} = 2$ and $r_o = 4$, for different values of N in the case of no noise ($p_{\boldsymbol{u}} = p_{\boldsymbol{t}} = 0$) and no regularization ($\mu_1 = \mu_2 = 0$). The maximum number of function evaluations was set to maxfev=10^5 and we fixed $\eta_{int} = 0.2, \eta_o = 2$. From the results presented in Figure 1, it appears that the MFS is highly accurate.

Next, in order to investigate the stability of the numerical solution, we fix $N = 64$ and include $p_{\boldsymbol{t}} = 5\%$ random noise in the input traction data (12). For simplicity, we consider no noise in the input displacement data (12), i.e. $p_{\boldsymbol{u}} = 0$. In Figure 2, we present the plots of the reconstructed boundary ∂D obtained with no regularization for various numbers of function evaluations nfev. Since the problem under investigation is ill-posed, when no regularization is employed, an unstable solution is expected and, from Figure 2, it can be observed that as nfev increases beyond a certain threshold so does the instability. In this case, in order to obtain a stable solution one needs to stop the iterative process at the first nfev at which the discrepancy principle (14) is satisfied. In Figures 3 and 4 we present plots of the reconstructed boundary of the rigid inclusion when regularization is included in (10), namely, $\mu_1 > 0$, $\mu_2 = 0$, and $\mu_1 = 0$, $\mu_2 > 0$, respectively. In comparison with Figure 2 where no regularization was employed, from Figures 3 and 4 it can be seen that improved stable results are obtained if regularization is

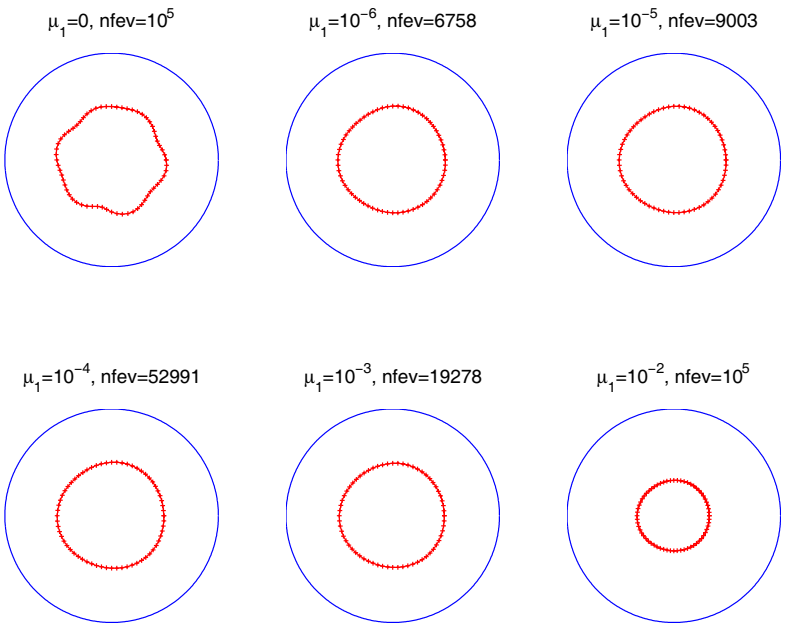

Figure 3: Results for various values of μ_1 with noise $p_{\boldsymbol{t}} = 5\%$ noise.

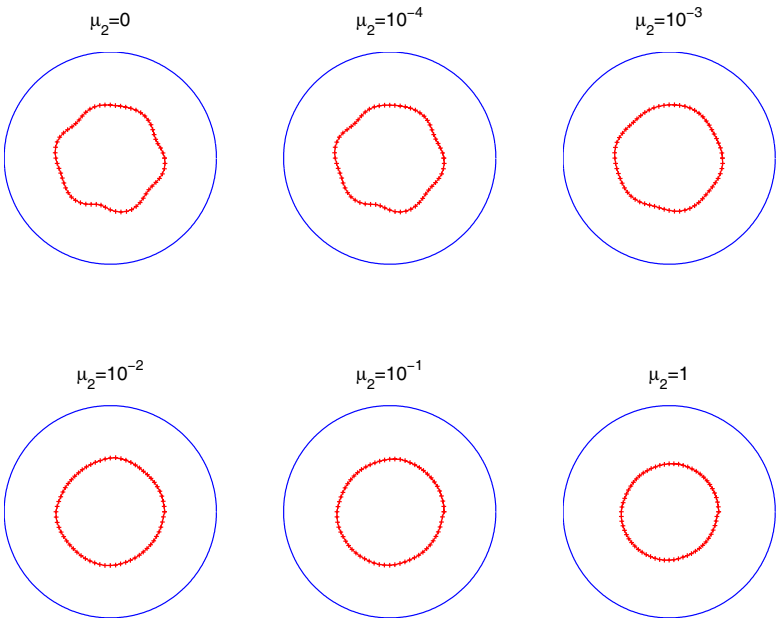

Figure 4: Results for various values of μ_2 with $p_{\boldsymbol{t}} = 5\%$ noise.

included. Interestingly, different values of the regularization parameter $\mu_1 > 0$ in Figure 3 had the effect of producing a number `nfev`, for which the convergence of (10) was reached, less than the prescribed $\texttt{maxfev} = 10^5$. Improved stable and accurate results were obtained for $\mu_1 = O(10^{-5}) \div O(10^{-3})$. In contrast, for various values of μ_2, `nfev` reached $\texttt{maxfev} = 10^5$. Even so, the numerical results obtained with $\mu_2 = O(10^{-3}) \div O(10^{1})$ in Figure 4 seem stable and reasonably accurate.

5 Conclusions

The MFS has been formulated for the solution of inverse inclusion problems arising in two-dimensional linear elasticity. The numerical experiments in the case of a rigid inclusion yield accurate results for exact data, but instabilities appear when noise is introduced into the input data. Regularization can be achieved either by appropriately limiting the number of functional evaluations, or by introducing penalty terms in the objective cost functional that is minimized. The extension of the proposed technique to inverse inclusion problems in three-dimensional linear elasticity, [15], is deferred to a future work.

References

[1] Fairweather, G. & Karageorghis, A., The method of fundamental solutions for elliptic boundary value problems. *Adv Comput Math*, **9**, pp. 69–95, 1998.
[2] Golberg, M.A. & Chen, C.S., The method of fundamental solutions for potential, Helmholtz and diffusion problems. *Boundary Integral Methods: Numerical and Mathematical Aspects*, ed. M.A. Golberg, WIT Press/Comput. Mech. Publ., Boston, MA, volume 1 of *Comput. Eng.*, pp. 103–176, 1999.
[3] Kołodziej, J.A. & Zieliński, A.P., *Boundary Collocation Techniques and their Application in Engineering*. WIT Press: Southampton, 2009.
[4] Ahmed, M.T., Lavers, J.D. & Burke, P.E., An evaluation of the direct boundary element method and the method of fundamental solutions. *IEEE Trans Magnetics*, **25**, pp. 3001–3006, 1989.
[5] Karageorghis, A., Lesnic, D. & Marin, L., A survey of applications of the MFS to inverse problems. *Inverse Probl Sci Eng*, 2011. To appear.
[6] Alves, C.J.S. & Martins, N.F.M., The direct method of fundamental solutions and the inverse Kirsch-Kress method for the reconstruction of elastic inclusions or cavities. *J Integral Equations Appl*, **21**, pp. 153–178, 2009.
[7] Marin, L., Regularized method of fundamental solutions for boundary identification in two-dimensional isotropic linear elasticity. *Int J Solids Struct*, **47**, pp. 3326–3340, 2010.

[8] Marin, L. & Johansson, B.T., Relaxation procedures for an iterative MFS algorithm for the stable reconstruction of elastic fields from Cauchy data in two-dimensional isotropic linear elasticity. *Int J Solids Struct*, **47**, pp. 3462–3479, 2010.
[9] Alessandrini, G., Bilota, A., Formica, G., Morassi, A., Rosset, E. & Turco, E., Numerical size estimates of inclusions in elastic bodies. *Inverse Problems*, **21**, pp. 133–151, 2005.
[10] Aliabadi, M.H., *The Boundary Element Method. Applications in Solids and Structures*. John Wiley and Sons: London, 2002. Volume 2.
[11] Martins, N.F.M. & Silvestre, A.L., An iterative MFS approach for the detection of immersed obstacles. *Eng Anal Bound Elem*, **32**, pp. 517–524, 2008.
[12] NAG(UK) Ltd, Wilkinson House, Jordan Hill Road, Oxford, UK, *Numerical Algorithms Group Library Mark 21*, 2007.
[13] Hansen, P.C., Regularization tools: a Matlab package for analysis and solution of discrete ill-posed problems. *Numer Algorithms*, **6**, pp. 1–35, 1994.
[14] Belge, M., Kilmer, M.E. & Miller, E.L., Efficient determination of multiple regularization parameters in a generalized L-curve framework. *Inverse Problems*, **21**, pp. 133–151, 2005.
[15] Marin, L., A meshless method for solving the Cauchy problem in three-dimensional elastostatics. *Comput Math Appl*, **50**, pp. 73–92, 2005.